

Mass Spectrometry

A Hybrid Orbitrap-Nanoelectromechanical Systems Approach for the Analysis of Individual, Intact Proteins in Real Time

Adam P. Neumann, Eric Sage, Dmitri Boll, Maria Reinhardt-Szyba, Warren Fon, Christophe Masselon, Sébastien Hentz, John E. Sader, Alexander Makarov, and Michael L. Roukes*

Abstract: Nanoelectromechanical systems (NEMS)-based mass spectrometry (MS) is an emerging technique that enables determination of the mass of individual adsorbed particles by driving nanomechanical devices at resonance and monitoring the real-time changes in their resonance frequencies induced by each single molecule adsorption event. We incorporate NEMS into an Orbitrap mass spectrometer and report our progress towards leveraging the single-molecule capabilities of the NEMS to enhance the dynamic range of conventional MS instrumentation and to offer new capabilities for performing deep proteomic analysis of clinically relevant samples. We use the hybrid instrument to deliver *E. coli* GroEL molecules (801 kDa) to the NEMS devices in their native, intact state. Custom ion optics are used to focus the beam down to 40 μm diameter with a maximum flux of 25 molecules/second. The mass spectrum obtained with NEMS-MS shows good agreement with the known mass of GroEL.

Introduction

Innovations in mass spectrometry (MS) instrumentation that combine high resolution, high mass accuracy, and high throughput have established the position of MS-based proteomics as the central technological paradigm driving the post-genomic era. The complete yeast proteome was quantified in 2008,^[1] and in 2014 two groups reported the first draft of the human proteome.^[2,3] In all cases, these analyses were performed using Orbitrap instrumentation. The Orbitrap™ mass analyzer,^[4] introduced in 2000, alleviated the shortcomings of previous analyzers, which suffered from deleterious factors such as poor transmission, low mass accuracy, low speed, or limited mass dynamic range.

Compared with genomic analysis, proteomics confronts a significant increase in both sample complexity and concentration dynamic range. Humans have approximately 20,000 genes^[2,3] that encode for millions of protein forms.^[5] Sample complexity is further compounded by proteolytic digestion and dissociation, which is commonly employed in “bottom-up” analysis to achieve accurate analyte identification via tandem MS spectra. A further complication is the immense dynamic range required for proteomics; the proteome of a HeLa cancer cell spans 8 orders-of-magnitude,^[6] while protein concentrations in the human plasma proteome span 11 orders of magnitude.^[7]

The complexity of proteomic samples is often addressed by employing liquid chromatography as an orthogonal separation technique at the front end. Meanwhile, there exists no protein analog to the polymerase chain reaction (PCR), which is used to amplify DNA and RNA to any quantity. Accordingly, to achieve deep and complete coverage of the proteome, analysis with single-protein resolution is essential. Additionally, at present MS is a single-channel methodology (providing just one analysis stream), for which Coulomb repulsion limits the number of molecules that can be processed simultaneously. The result is that mass spectrometers, including those using Orbitrap technology, fall five to six orders-of-magnitude short on dynamic range needed for deep proteome analysis of clinically relevant samples. Current studies analyzing the deep proteome are thus ensemble averages, performed on large samples of cell clones.^[6]

Consider a hypothetical enhancement to MS instrumentation that increases the dynamic range to the theoretical

[*] A. P. Neumann, E. Sage, W. Fon, M. L. Roukes
 Kavli Nanoscience Institute and Department of Physics,
 California Institute of Technology, Pasadena, California 91125, USA
 E-mail: roukes@caltech.edu

D. Boll, M. Reinhardt-Szyba, A. Makarov
 Thermo Fisher Scientific,
 28199 Bremen, Germany

C. Masselon
 Univ. Grenoble Alpes, CEA, IRIG, Biologie à Grande Echelle,
 INSERM UA 13, F-38054 Grenoble, France

S. Hentz
 Univ. Grenoble Alpes, CEA, Leti, F-38000 Grenoble, France

J. E. Sader
 Graduate Aerospace Laboratories and Department of Applied
 Physics, California Institute of Technology,
 Pasadena, California 91125, USA

A. Makarov
 Biomolecular Mass Spectrometry and Proteomics, Bijvoet Center
 for Biomolecular Research and Utrecht Institute for Pharmaceutical
 Sciences, University of Utrecht,
 Padualaan 8, 3584 CH Utrecht, The Netherlands

M. L. Roukes
 Departments of Physics, Applied Physics and Bioengineering,
 California Institute of Technology,
 Pasadena, California 91125, USA

limit. This would allow for the entire proteome from a small sample, such as that acquired from a single cell, to be readily analyzed within a reasonable timeframe. This enhancement could take the form of a device or intermediate analyzer that examines molecules one-by-one. Here, we report on progress towards the first generation of such an instrument, achieved by concatenating a NEMS array behind an Orbitrap mass spectrometer.

Nanoelectromechanical Systems (NEMS) are devices that integrate mechanical functionality with electrical detection to enable physical measurements on objects of nanometer dimensions. Unlike conventional mass spectrometry, NEMS devices enable measurement of mass via changes in their mechanical properties; in particular, by resolving the shift in resonance frequency induced when an individual analyte physisorbs upon the device surface. NEMS are typically constructed from materials such as monocrystalline silicon or silicon carbide. Electron beam lithography along with nanofabrication processes are used to form simple resonant structures such as miniature plates, cantilevers, or beams, or more complex devices that include phononic band gap isolation, with typical feature sizes of order tens of nanometers to micrometers. These devices exhibit attributes that merit their consideration for MS: most notably, their extreme sensitivity to the addition of single molecules, and their mass resolution, which actually increases with increased mass within their mass dynamic range that extends well into the hundreds of MDa regime.^[8–13] This contrasts markedly with other approaches.

The minute mass of these fabricated structures enables the detection of tiny added particles, such as nanoparticles, individual proteins, protein complexes, and large biomolecules in the hundreds of kDa to multiple MDa range,^[19,20] and intact viruses in the multiple MDa range.^[14–18] NEMS also offer promise for single-Dalton resolution of protein species.^[21–23] The principle behind NEMS-MS lies in driving mechanical devices at resonance and monitoring the changes induced in their resonance frequencies in real time as individual analytes physisorb upon their surface.^[19] The abrupt change in frequency shifts that occur with each adsorption event can thus be used to calculate the mass of each individual particle.

The uncertainty in measured mass σ_m and the minimum detectable mass of these devices is proportional only to the frequency fluctuations σ_f from which the aforementioned frequency shifts are extracted. Reducing σ_m is achieved by operating the NEMS under vacuum and cryogenic temperatures. Over the measurement integration time chosen to optimally extract frequency shifts, these fluctuations are observed to remain relatively constant for each device. Accordingly, the mass uncertainty of each analyte measured is independent of its mass. In fact, the value m/σ_m (referred to as resolution or resolving power) actually *increases* with mass, making NEMS-MS particularly suitable for high mass species.

NEMS-MS does not inherently require ionization of analytes. Experimental realizations of neutral-particle detection with NEMS^[19,24] demonstrate they can circumvent issues associated with ion transfer efficiency or heterogeneous

peak structure^[25] associated with typical MS measurements. NEMS devices are poised to outperform traditional MS in the MDa mass range, where traditional MS faces challenges.^[25] Significant developments in the field of Native MS,^[26] which permit analysis of protein complexes in their intact state, have dramatically extended the mass range of Orbitrap analysis, up to the scale of large protein complexes and viruses,^[27–29] although analyte throughput is limited.

Our prior instantiations of NEMS technology have utilized custom ion optics and vacuum systems to direct molecules to the NEMS, recreating traditional MS-based instrumentation *de novo*.^[8,15] These first instruments demonstrated relatively low ion flux due to the mismatch between the typical ion beam size of a few square mm and the cross-section of a typical NEMS resonator at a few square μm . Work to increase the capture cross section of the ion beam has been demonstrated with arrays of up to 20 NEMS devices,^[30] with the possibility of arrays of tens-of-thousands of devices produced *en masse* utilizing VLSI fabrication techniques.^[41] Alternatively, ion optics can be used to significantly shrink the beam size and to implement scanning of multiple devices; this permits a single NEMS device to capture a significant fraction of the analytes that approach it.

Here, we demonstrate the use of an Orbitrap based mass spectrometer to deliver individual, intact *E. coli* GroEL (801 kDa) molecules, a noncovalent protein complex consisting of 14 identical subunits, to an array of 20 NEMS resonators that can each measure the analyte mass one molecule at a time. Ion optics designed to focus the beam of GroEL ions to a spot size of 50 μm are manufactured and incorporated into the hybrid instrument. The NEMS array is used to precisely map the ion flux in three dimensions. The map thus obtained matches the predicted focusing capability and is used to find the optimal location for NEMS operation. An inertial mass spectrum of GroEL is compiled from each individual absorption event and the measured mass shows excellent agreement with its expected value. We discuss future work that will enable the practical use of NEMS in modern MS instrumentation to extend its capabilities.

Results and Discussion

An overview of the instrument is shown in Figure 1. A Thermo Scientific™ Q Exactive™ Plus instrument with Orbitrap detection capable of analyzing the mass-to-charge ratio of species with extremely high resolving power (up to 140,000 for 200 m/z)^[31] is modified with extended mass range (EMR) capabilities and a special quadrupole for selecting the species of interest. The front end is outfitted with an electrospray ionization (ESI) or nanoelectrospray (nano-ESI) ionization source, thus providing an interface for transferring molecular species from solution to the gas phase. This is compatible with standardized protocols used in proteomics or native mass spectrometry research. A similar instrument was previously constructed and reported measurement of intact IgG antibody at 149 kDa, yeast

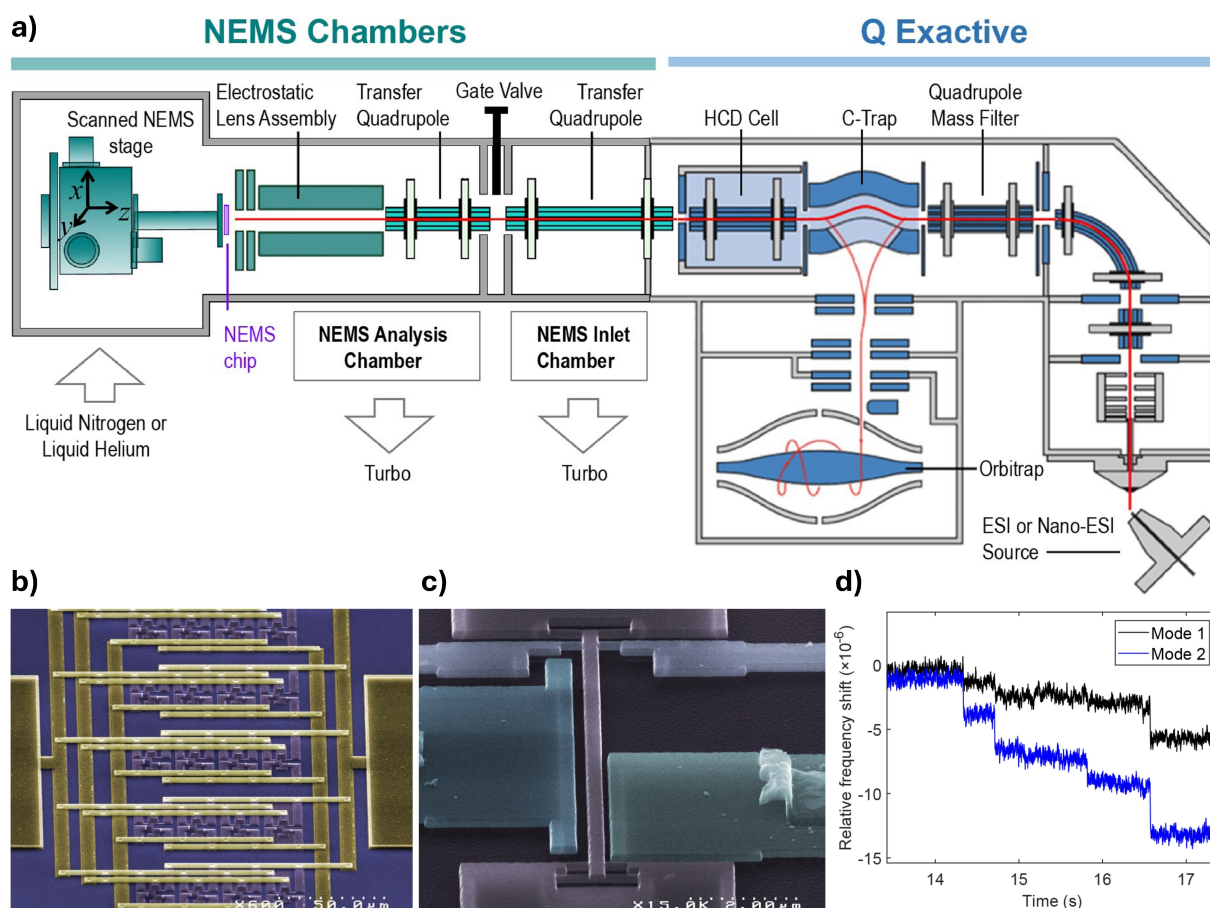


Figure 1. Real-time detection of GroEL adsorbed onto doubly clamped NEMS beams in high vacuum. **a)** Architecture of the Hybrid Q Exactive-NEMS System that delivers intact proteins or protein complexes to the Orbitrap chamber for analysis of mass-to-charge ratio and then onto the NEMS for single molecule analysis. **b)** SEM image of a 20-device array of doubly clamped beams shown with silicon, colored in deep blue, and the metallization layers (Al:Si), colored in yellow, used to interconnect the electrical connections of each resonator. **c)** Zoom-in on single in-plane resonator used in this study with colorized actuation gates and bias electrodes. **d)** As GroEL adsorbs onto a NEMS resonator, the resonance frequency of each tracked resonant mode abruptly shifts, and this shift in resonant frequency is observed in real time.

proteasome at 730 kDa, and GroEL at 801 kDa,^[27] and up to viral nanoparticles at 4.5 MDa.^[28]

Successful realization of the hybrid system requires careful modification of the design of the Q Exactive MS and provision of the requisite operating conditions of both the Q Exactive and the NEMS devices. The Q Exactive MS includes multiple chambers for transferring or trapping ions. One such chamber, the higher-energy collisional dissociation (HCD) cell, includes a removable back port that facilitates our instrument modifications.

Figure 1 provides a schematic overview of the instrumentation. An additional vacuum chamber (NEMS Inlet Chamber) is attached to the HCD cell after removing its back plate, followed by a gate valve and a second vacuum chamber (NEMS Analysis Chamber). The use of two chambers allows for differential pumping to maintain the proper vacuum regime for the HCD cell, the Q Exactive MS, and the NEMS chamber, as well as providing straightforward NEMS device exchange without breaking the vacuum of the Q Exactive MS. The HCD cell in the Q Exactive MS acts as an extended trapping region for larger

molecular weight complexes. Relatively high pressure (10^{-2} Torr) is used in this chamber, both to trap incoming ions (so they can be collected in the C-Trap prior to injection into the Orbitrap) and to remove excess water and salt molecules via collisions with gas molecules.^[27] In contrast, NEMS operation requires low pressure (10^{-6} Torr). While dissipation of NEMS devices due to collisions with gas molecules becomes negligible at pressures less than a few mTorr,^[32] a larger concern is the possibility of significant adsorption of ambient gas while operating the devices at cryogenic temperatures. Such adsorption would lead to a constant drift in resonance frequency of the devices and enhancement of fluctuation processes that degrade their noise performance.^[33,34] A CAD model of the system is provided in Supporting Information Figure S1, and images of the exterior and interior are provided in Supporting Information Figure S2.

With this design, the NEMS analysis chamber is maintained at a steady pressure of 3×10^{-7} Torr, regardless of the pressure in the HCD cell. The end-to-end gap between transfer quadrupoles is set to 5 mm to avoid excessive loss of

ion transfer efficiency, and a miniature gate valve (VAT) with a gate thickness of 4 mm is available to make this possible. The NEMS chip itself is mounted on a printed circuit board that rests on a XYZ piezoelectric translation stage (Attocube) that provides 5 mm of travel range with sub-nanometer positioning precision along the three axes. It is thermalized to a flow cryostat (Janis), which is cooled with liquid nitrogen. The system can reach a base temperature of 80 K within 20 hours; cryogenic design and temperature readings are provided in Supporting Information Figure S3.

A critical design criterion is achieving sufficient ion flux to the NEMS. The typical cross section for devices used for mass sensing is of order of $10\ \mu\text{m}$ by $0.3\ \mu\text{m}$, which represents an extremely small capture cross section for typical ion beam sizes of order of a few square mm. This previously presented a major barrier to obtaining enough physisorption events to permit adequate measurement statistics; to wit, an early ESI based instrument achieved a maximum rate of only 1 event per minute.^[35] This limitation is surmounted here with the addition of ion optics immediately prior to the NEMS, which greatly increases the analyte flux density delivered to the NEMS. Our design for a two-stage ion lens focusing the ions to a spot size of $50\ \mu\text{m}$ is shown in Figure 2.

Custom instrument control software is used to either trap ions in the HCD cell prior to injecting them into the Orbitrap analyzer or to allow the ions to continue through the HCD cell to the NEMS. The choice of path can be adjusted rapidly, allowing for Orbitrap m/z spectra to be associated with NEMS measurements and validate which molecules are being sent to the NEMS. GroEL molecules are ionized using the nano-ESI source (see SI), and the quadrupole mass-filter board was modified to filter mole-

cules with m/z greater than 10,000. As shown in Supporting Information Figure S4, a mass spectrum collected using the Orbitrap analyzer is similar to results reported elsewhere.^[27] The mass spectrum confirms the GroEL molecules retain their intact 14-mer configuration with a calculated mass of 801.421 kDa, and the use of the quadrupole filter prevents fragments or other contaminants from reaching the NEMS.

Our initial NEMS measurements required significant effort to locate the ion beam, given its tight focusing implemented in this work. Prior to collecting significant data for MS, we systematically characterize in three dimensions the ion beam directed toward the NEMS. A 20-device NEMS array is used for this purpose, which greatly increases the throughput of data collection. A schematic diagram of the NEMS array operation is provided in Supporting Information Figure S5, and the electronic operation and readout Scheme is provided in Supporting Information Figure S6. Additional details concerning the operation and fabrication of this array are provided in Ref. [30]. In brief, the devices have a pitch of $20\ \mu\text{m}$ in X and $60\ \mu\text{m}$ in Y for a total field size of $60\times 240\ \mu\text{m}$. Devices are $160\ \text{nm}$ thick by $300\ \text{nm}$ wide; the lengths vary from $7\text{--}9.2\ \mu\text{m}$. Each device possesses five electrical connections. They are interconnected in parallel using two additional metal layers. This ensures that the input signal is applied to all NEMS simultaneously, and the overall output is the sum of all individual outputs of the devices. Because the device resonance frequencies are different, they are separately frequency-addressable. The entire array is monitored by sequentially switching between the resonance frequency of each resonator: a phase-locked loop (PLL) locks onto a given resonator using its last known resonance frequency, registers its current resonance frequency after a given idling

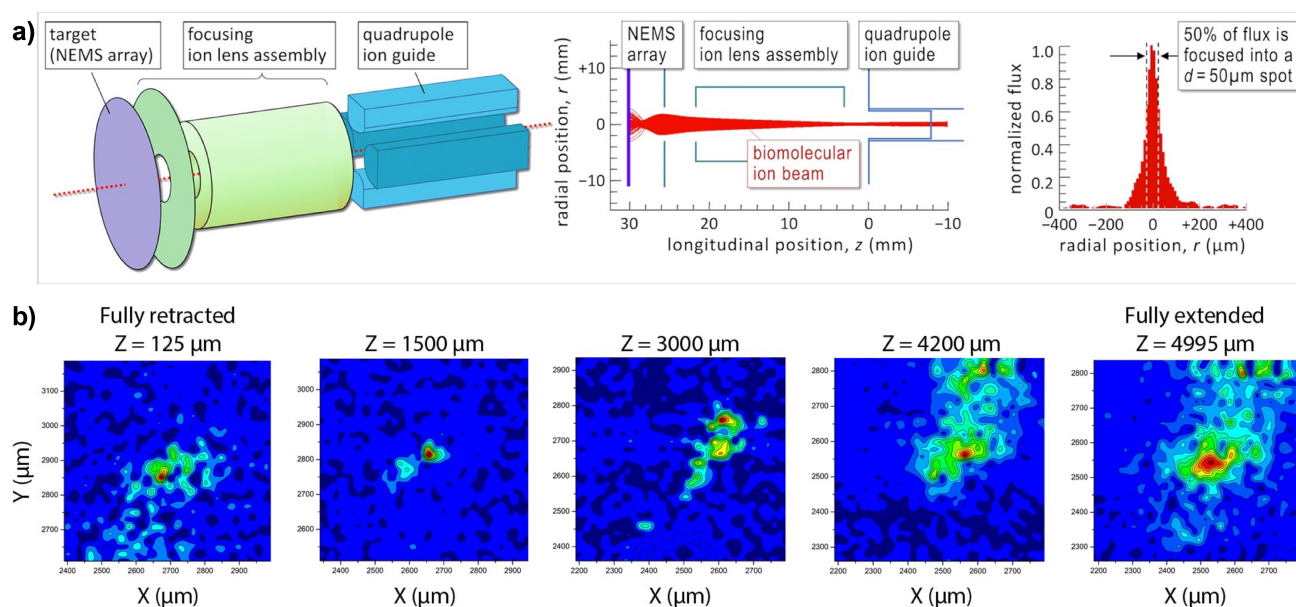


Figure 2. Ion optics and high-resolution map of three-dimensional ion flux. (A) A series of ion lenses were designed to focus the ion beam exiting the Q Exactive MS into a $50\ \mu\text{m}$ spot. (B) 3D map of ion flux obtained by extending or retracting the positioner in the Z direction (along the ion beam) and scanning the NEMS array in X and Y (transverse to the ion beam) such that a data point is obtained every $20\ \mu\text{m}$. The most focused position in the second Figure has a spot size of $40\ \mu\text{m}$ with a peak flux of roughly 25 molecules per second.

time, τ (here 10 ms), and then switches to the next resonator. Frequency time traces for each individual device are extracted after the experiment. Data displaying frequency-tracking of myoglobin molecular adsorption events to each device of the array is shown in Supporting Information Figure S7.

To map the ion flux of GroEL in three dimensions, we use the 3D XYZ positioner's capability for 0.1 nm positioning precision over a 5 mm travel range. The array has a pitch of 20 μm in X and 60 μm in Y. Therefore, to achieve uniformly spaced data collection, the array is first staggered twice in Y by 20 μm , forming a field of 60 \times 300 μm with a data point every 20 μm in X and Y. This is then repeated to form a field of 600 \times 600 μm perpendicular to the ion beam axis. This is done with 3 minutes spent per position, so each field takes 1 hour to capture. Finally, it is repeated for several Z values, from fully retracted (further from the lens, Z=125 μm) to fully extended (closer to the lens, Z=4995 μm). Positioning is performed in an automated manner using a custom Python script.

Results are shown using contour plots in Figure 2 with raw data given in terms of the NEMS relative frequency shift per second. This can be converted to molecules per second using the mass responsivity for mode 1 of the NEMS at 12 Hz/ag, or the responsivity for mode 2 (not shown) at 32 Hz/ag,^[30] with the approximate respective NEMS resonance frequencies of 25 and 67 MHz, and a GroEL mass of 1.3 ag. The ions are focused to a minimum beam size of 40 μm , with a maximum flux rate of 25 molecules per second. Such data, once collected, is useful for finding the ions again after installing a new NEMS device, as well as setting the position of the device to achieve the desired flux rate. A similar map is obtained with myoglobin ions demonstrating a maximum flux of 880 molecules per second (SI, Figure S8).

Following characterization of the ion beam with a 20-device array, the smallest device in the array (7 μm length) with the lowest (best) mass resolution is operated in isolation at a location within the focused ion beam that provides an event rate of ~ 1 molecule per second. This rate is chosen to demonstrate the ability to collect a large amount of data in a short period of time, while still having a low probability of multiple molecules landing within the measurement window of 200 ms. This measurement window is set according to the PLL loop integration time (measurement time) that minimizes the Allan deviation, which is measured to be 2.2×10^{-7} for mode 1 and 1.8×10^{-7} for mode 2 (with a noise correlation of $\rho=0.28$), corresponding to an expected mass resolution of ~ 118 kDa.

Jumps are automatically detected and evaluated to build a mass spectrum using our previously reported methods.^[8,24] For a 1D doubly-clamped Euler-Bernoulli beam, the frequency shifts of the resonant modes obey:

$$\frac{\delta f_n}{f_n} \approx -\frac{m_{\text{added}}}{2M_{\text{device}}} \phi_n^2(x), \quad (1)$$

where δf_n is the change in resonant frequency of the device upon mass adsorption, f_n is the resonant frequency of the

device without the adsorbate, m_{added} is the adsorbed mass at position x , M_{device} is the device mass, and $\phi_n(x)$ is the scaled displacement mode shape of mode n ; Eq. (1) is valid for $m_{\text{added}} \ll M_{\text{device}}$. As shown in Eq. (1), the frequency shifts depend not only on mass but also the (unknown) position where the particle lands. For the doubly-clamped beams used in this study, measurement of the first two vibrational modes of the device is sufficient to determine not only the unknown position, but also the mass of each particle.^[8] The calculation of the mass spectrum relies on this formula as well as a probability density based formulation through a change of variables that transforms measured frequency shifts and their uncertainties into mass and position and their uncertainties.^[35] Adsorption events are identified as fluctuations that exceed a 5σ deviation from background noise, which for the first two modes is observed to form a bivariate normal distribution over a given measurement window. Further details of obtaining the mass spectrum are provided in SI. The mass spectrum features a primary peak at 748 kDa, close to the known mass of 801 kDa and a series of smaller, unresolved secondary peaks at higher mass (Figure 3). While this mass difference (~ 53 kDa) is close to that of a single GroEL subunit (~ 57 kDa), previous native mass spectrometry investigations of this molecule, under similar analysis conditions, did not show such fragmentation.^[36] Instead, we attribute the mass difference observed here to our uncertainties ($\sim 5\%$) in establishing the modal masses of the NEMS devices; accurate knowledge of them is required to deduce analyte mass precisely.

A simulation used to validate the experimentally obtained spectrum is performed as follows. An 801 kDa point mass is adsorbed with random position to a 1D doubly clamped beam. The frequency shifts of the resonant modes are calculated according to Eq. (1) for each simulated adsorption event, then noise is sampled from the experimentally obtained noise distribution for the chosen measurement window and added to the (noise-free) modelled frequency shifts. A mass spectrum is then obtained using 1000 such events according to the same procedure in SI. The peak of the simulated spectrum matches the simulation input of 801 kDa. However, the width of the simulated spectrum, measured by the full width at half maximum (FWHM) is 278 kDa (Figure 3), significantly smaller than the experimentally obtained spectrum, measured at 445 kDa.

The relatively broad observed peak compared with the simulation is unlikely to be due to variation in sample mass. This is because the hybrid Orbitrap-NEMS instrument allows for selection of only intact GroEL molecules using the quadrupole mass filter and validation of the intact nature using the Orbitrap analyzer (SI, Figure S4). A doublet, or two GroEL molecules arriving at a single position and at the same time, should produce a clearly resolvable peak at twice the main peak, given the device resolution. This is not observed in the measured spectrum. One possibility is a significant fraction of events consist of multiple particles landing at different positions within the chosen measurement interval of 200 ms. Such multiple-jump events violate the assumptions of the probability distribution framework detailed in the Supporting Information Materials

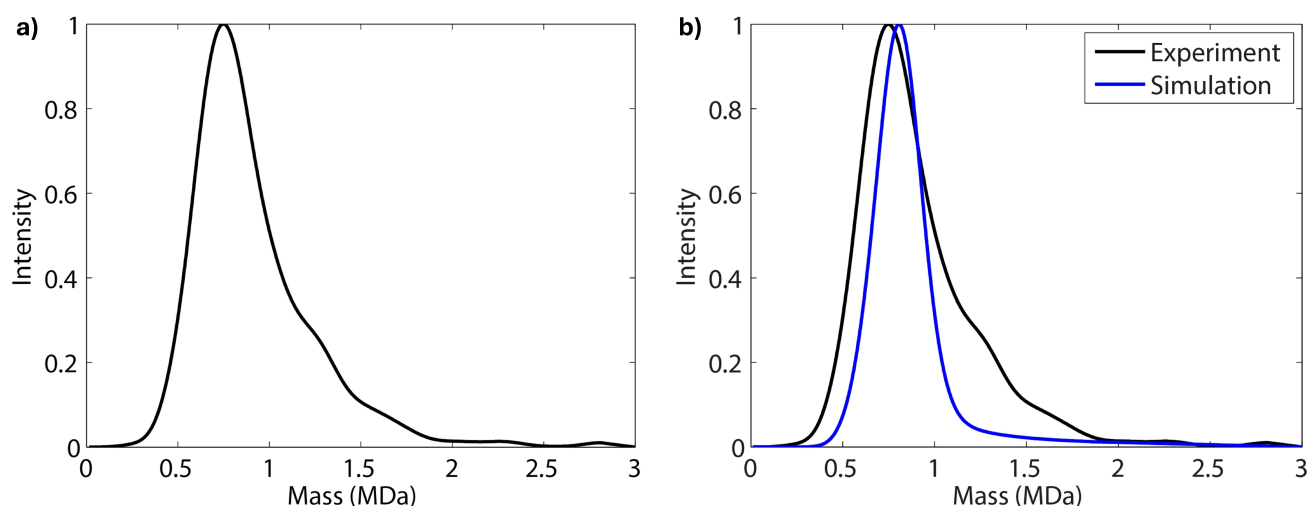


Figure 3. GroEL inertial mass spectrum and simulated spectrum. a) NEMS-MS spectrum of GroEL with a primary peak at 748 kDa and unresolved secondary peaks at higher mass. b) A simulation matching details of the experiment is shown alongside the observed mass spectrum; see text for details. In the simulation, the adsorption events are independent, and the mass spectrum features a single, narrower peak.

and would broaden the final mass spectrum. This could occur if the true event rate is faster than the estimated 1 molecule per second, or if the molecules do not arrive at a fixed rate but instead in bunches. Additional work to resolve multiple-landing events through use of an improved event-detection scheme, or the use of additional modes to detect the presence of multiple particles^[37] will be used in further studies that employ a high event rate.

Conclusions

The hybrid instrument we describe here makes it possible to perform several important experiments. It enables Orbitrap-based verification of the GroEL ions sent to NEMS devices, and direct resolution of single-molecule adsorption events and subsequent deduction of analyte mass. Mass spectra collected with two simultaneous modes show good agreement with the expected mass. Ion optics is used to produce a beam with a diameter of 40 μm ; this yields a maximum detection rate of 25 molecules per second for GroEL and 880 molecules per second for myoglobin. Using a 20-device array, consisting of 10 μm by 300 nm devices, currently permits detection of 5 % of the total molecular flux reaching the device chip. This indicates that NEMS can enable a very low limit of detection, that is, a low number of molecules in the initial solution needed to produce a signal. Other factors affecting the detection limit using NEMS are solely the electrospray ionization efficiency (typically 5–10 %, with the theoretical limit up to 85 %)^[38] and the transfer efficiency of ions to the NEMS (estimated to be 13 % for this hybrid instrument with further details in Ref. [39]). Thus, we estimate that the current detection limit achieved is of order 10^4 to 10^5 molecules. This enables proteomic experiments on extremely small sample sizes, such as that from a single cell.

To achieve significant improvement to existing NEMS-MS instruments, two orders enhancement of mass resolution

are needed, along with controlled desorption of individual molecules from the NEMS devices. We anticipate that the former is within reach with next-generation phononic band gap NEMS devices with ultralow energy dissipation.^[40,41] These are of sufficient size to permit analysis of large protein complexes, while also potentially yielding single Dalton mass resolution. Experiments are underway to explore both soft landing of individual protein analytes on the NEMS as well as their controlled desorption.

Author Contributions

M.L.R. and A.A.M. conceived of and directed this effort. A.P.N., E.S., and W.F. built the nanosystems instrumentation and carried out the experiments. D.B., M.R.-S., and A.A.M. designed the specialized ion optics and provided expertise on MS operations. C.M. and S.H. provided NEMS devices and advice on experiments. A.P.N., J.E.S. and M.L.R. analyzed the data. All authors discussed the results and edited the paper.

Acknowledgements

The authors gratefully acknowledge support from the Wellcome Leap Foundation through its Delta Tissue program, the National Science Foundation (Major Research Instrumentation Award 1828787 and Partnerships for Innovation Award 2016555), and an Amgen Chem-Bio-Engineering Award (CBEA). We also thank Prof. Albert Heck and his laboratory (Utrecht Univ., NL) for helpful discussions and provision of the GroEL samples analyzed.

Conflict of Interest

D.B., M.R.-S. and A.A.M. are employees of Thermo Fisher Scientific, which commercializes Orbitrap-based instruments for MS.

Data Availability Statement

The data that support the findings of this study are available from the corresponding author upon reasonable request.

Keywords: Nanomechanical systems · mass spectrometry · native mass spectrometry

- [1] L. M. De Godoy, et al. *Nature* **2008**, 455, 1251–1254.
- [2] M.-S. Kim, et al. *Nature* **2014**, 509, 575–581.
- [3] M. Wilhelm, et al. *Nature* **2014**, 509, 582–587.
- [4] A. Makarov, *Anal. Chem.* **2000**, 72, 1156–1162.
- [5] W. C. Cho, *Genomics Proteomics Bioinf.* **2007**, 5, 77–85.
- [6] N. Nagaraj, et al. *Mol. Syst. Biol.* **2011**, 7, 548–548.
- [7] N. L. Anderson, *Mol. Cell. Proteomics* **2002**, 1, 845–867.
- [8] M. S. Hanay, et al. *Nat. Nanotechnol.* **2012**, 7, 602–608.
- [9] K. L. Ekinici, X. M. H. Huang, M. L. Roukes, *Appl. Phys. Lett.* **2004**, 84, 4469–4471.
- [10] B. Ilic, et al. *J. Appl. Phys.* **2004**, 95, 3694–3703.
- [11] Y. T. Yang, C. Callegari, X. L. Feng, K. L. Ekinici, M. L. Roukes, *Nano Lett.* **2006**, 6, 583–586.
- [12] M. Li, H. X. Tang, M. L. Roukes, *Nat. Nanotechnol.* **2007**, 2, 114–120.
- [13] E. Gil-Santos, et al. *Nat. Nanotechnol.* **2010**, 5, 641–645.
- [14] C. Y. Chen, et al. *Nat. Nanotechnol.* **2009**, 4, 861–867.
- [15] A. K. Naik, M. S. Hanay, W. K. Hiebert, X. L. Feng, M. L. Roukes, *Nat. Nanotechnol.* **2009**, 4, 445–450.
- [16] S. Schmid, M. Kurek, J. Q. Adolphsen, A. Boisen, *Sci. Rep.* **2013**, 3, 1288.
- [17] T. P. Burg, et al. *Nature* **2007**, 446, 1066–1069.
- [18] A. Gupta, D. Akin, R. Bashir, *Appl. Phys. Lett.* **2004**, 84, 1976–1978.
- [19] S. Dominguez-Medina, et al. *Science* **2018**, 362, 918–922.
- [20] R. T. Erdogan, et al. *ACS Nano* **2022**, 16, 3821–3833.
- [21] K. Jensen, K. Kim, A. Zettl, *Nat. Nanotechnol.* **2008**, 3, 533–537.
- [22] H. Y. Chiu, P. Hung, H. W. Postma, M. Bockrath, *Nano Lett.* **2008**, 8, 4342–4346.
- [23] B. Lassagne, D. Garcia-Sanchez, A. Aguasca, A. Bachtold, *Nano Lett.* **2008**, 8, 3735–3738.
- [24] E. Sage, et al. *Nat. Commun.* **2015**, 6, 1–5.
- [25] E. van Duijn, *J. Am. Soc. Mass Spectrom.* **2010**, 21, 971–978.
- [26] A. J. R. Heck, *Nat. Methods* **2008**, 5, 927–933.
- [27] R. J. Rose, E. Damoc, E. Denisov, A. Makarov, A. J. Heck, *Nat. Methods* **2012**, 9, 1084–1086.
- [28] J. Snijder, et al. *J. Am. Chem. Soc.* **2014**.
- [29] T. P. Wörner, et al. *Nat. Chem.* **2022**, 14, 515–522.
- [30] E. Sage, et al. *Nat. Commun.* **2018**, 9, 3283.
- [31] Technical Information for Thermo Scientific Q Exactive Plus Orbitrap LC–MS/MS System, **2018**.
- [32] K. L. Ekinici, M. L. Roukes, *Rev. Sci. Instrum.* **2005**, 76, 061101.
- [33] Y.-T. Yang, *California Institute of Technology*, **2006**.
- [34] Y. T. Yang, C. Callegari, X. L. Feng, M. L. Roukes, *Nano Lett.* **2011**, 11, 1753–1759.
- [35] M. S. Hanay, *California Institute of Technology*, **2011**.
- [36] E. van Duijn, *Utrecht University*, **2006**.
- [37] J. E. Sader, et al. *Nano Lett.* **2018**, 18, 1608–1614.
- [38] R. B. Cole, *John Wiley & Sons*, **2011**.
- [39] A. P. Neumann, *California Institute of Technology*, **2020**.
- [40] P. Arrangoiz-Arriola, et al. *Nature* **2019**, 571, 537–540.
- [41] E. A. Wollack, et al. *Appl. Phys. Lett.* **2021**, 118, 123501.

Manuscript received: November 10, 2023

Accepted manuscript online: May 20, 2024

Version of record online: June 25, 2024